Neutrino-nucleus interaction rates at a low-energy beta-beam facility

Julien Serreau[*]

Institut für Theoretische Physik der Universität Heidelberg,
Philosophenweg 16, D-69120 Heidelberg, Germany

Cristina Volpe[†]

Institut de Physique Nucléaire, F-91406 Orsay Cedex, France
(Dated: April 30, 2004)

We compute the neutrino detection rates to be expected at a low-energy beta-beam facility. We consider various nuclei as neutrino detectors and compare the case of a small versus large storage ring.

PACS numbers: 25.30.Pt, 26.50.+x

The pioneering experiment of R. Davis [1] has started the era of neutrino astronomy. Because they only have weak interactions with matter, neutrinos are precious messengers of what happens in the interior of stars, like our sun, or in explosive phenomena, such as Supernova type II explosions. Such astronomical neutrinos therefore provide an important source of information for our understanding of the life (and death) of stars. Nuclei are commonly used as detectors in neutrino observatories as well as in various experiments aiming at studying intrinsic neutrino properties, such as their masses, and mixings. A precise knowledge of neutrino-nucleus cross-sections is needed for the interpretation of these measurements and/or to study the feasibility of new projects. The understanding of neutrino-nucleus interactions is also of crucial importance for various astrophysical processes. A timely example is that of the nucleosynthesis of heavy elements during the so-called r-process. If the latter takes place during the explosion of Supernovae type II, where a gigantic amount of energy is emitted as neutrino of all flavors, final abundances depend on several nuclear properties, among which the interactions with neutrinos [2–8].

Neutrinos emitted from core-collapse supernovae have typical energies of several tens of MeV. In the detection on earth, they have impinging energies from ten MeV for reactor and solar neutrinos, to the GeV and multi-GeV range for atmospheric neutrinos and long-baseline experiments. The various theoretical approaches employed to describe neutrino-nucleus interactions therefore involve from nuclear to nucleonic degrees of freedom (for a review, see [9]). There are a number of open issues in this context. The A=2 system is the simplest case, for which the reaction cross sections can be estimated with high accuracy [10]. However, there is still an important quantity, namely $L_{1,A}$, related to the axial two-body current, which dominates the theoretical uncertainty in neutrino-deuteron interactions. For heavier nuclei, in the tens of MeV energy range, the reaction cross sections are dominated by collective modes, like the Gamow-Teller resonance or the Isobaric Analog State, which have been extensively studied in the past [11]. As the neutrino impinging energy increases, transitions to states of higher multipolarity (such as the spin-dipole or higher forbidden transitions) become important [12]. The latter also play an important role in the context of core-collapse supernova physics [4, 12, 13]. However, the experimental information on these states is rather scarce. Note that the understanding of neutrino-carbon reactions with neutrinos produced from the decay in flight of pions is still an open issue, for most of the theoretical calculations overestimate the experimental value [14]. So far, measurements with low-energy neutrinos have been performed in a few cases only, namely deuteron [15], carbon [16], and iron [17]. Systematic studies would be of great importance both for what concerns the interpolation from the MeV to the GeV neutrino energy range and the extrapolation to neutron-rich nuclei, as required in the astrophysical context.

Neutrino-nucleus interaction studies were one of the main physics issues of the proposed ORLAND underground neutrino facility, which was based on a conventional neutrino source (pion and muon decays) [18]. At present, the MINERνA project [19] includes the study of neutrino-nucleus interactions for neutrino energies in the GeV range. Here, we study the potential of a low-energy neutrino facility based on beta-beams, a novel method to produce neutrino beams. This consists in boosting exotic ions which decay through beta-decay and produce pure, collimated and well-understood electron neutrino fluxes. Such method could be exploited for a future facility at CERN [20, 21]. High energy beta-beams would be fired to a gigantic Cherenkov detector like UNO [22], located in an (upgraded) Fréjus underground laboratory to study, in particular, the possible existence of CP violation in the leptonic sector [20, 21, 23]. The discovery potential with a very high γ and a longer baseline is discussed in [24].

It has recently been proposed to use the beta-beam concept for the production of low-energy neutrinos [25]. Several laboratories will produce intense exotic beams in the near future and could, therefore, be possible sites for

[*]Electronic address: `serreau@thphys.uni-heidelberg.de`
[†]Electronic address: `volpe@ipno.in2p3.fr`

a low-energy beta-beam facility. These include GANIL, CERN, GSI, as well as the EURISOL project. Low-energy neutrino beams would offer an interesting opportunity to study various neutrino properties, such as e.g. the neutrino magnetic moment [26], as well as neutrino-nucleus interactions, of interest for nuclear physics, particle physics and astrophysics. In the former case, one would exploit the ions at rest as an intense neutrino source, whereas, in the latter case, one would use boosted ions, which would be stored in a storage ring [25], as in the original high energy proposal. An important feature of such beta-beams is that the boost factor of the accelerated ions can be varied, allowing one to explore various neutrino energy ranges.

In this letter, we present for the first time charged-current neutrino-nucleus interaction rates achievable at a low-energy beta-beam facility. We consider two possible cases for the dimensions of the storage ring, for which we inspire ourselves of the one planned in the GSI upgrade [27] and the one thought in the CERN baseline scenario [20, 21]. We consider various target nuclei as neutrino detectors, namely deuteron, oxygen, iron and lead, which are commonly used in existing or planned experiments [18].

I. CALCULATIONS OF THE NEUTRINO FLUXES AND INTERACTION RATES

The decay rate of a nucleus in the rest (cm) frame can be written as:

$$\frac{dW}{dt}\bigg|_{cm} = \Phi_{cm}(E_\nu)\, dE_\nu\, \frac{d^2\Omega}{4\pi}\,, \qquad (1)$$

where E_ν and Ω denote respectively the energy and the solid angle of the emitted (anti-)neutrino, and where the neutrino flux $\Phi_{cm}(E_\nu)$ is given by the well-known formula [28]:

$$\Phi_{cm}(E_\nu) = b\, E_\nu^2\, E_e\, \sqrt{E_e^2 - m_e^2}\, F(\pm Z, E_e)\, \Theta(E_e - m_e)\,. \qquad (2)$$

where the constant $b = \ln 2/m_e^5 f t_{1/2}$, with m_e the electron mass and $f t_{1/2}$ the ft-value. The quantities appearing in the above expression are the energy $E_e = Q - E_\nu$ of the emitted lepton (electron or positron), Q being the $Q-$value of the reaction, and the Fermi function $F(\pm Z, E_e)$, which accounts for the Coulomb modification of the spectrum.

In the laboratory frame, where the boosted nucleus has a velocity $v = \beta c$, the decay rate reads:

$$\frac{dW}{dt}\bigg|_{lab} = \frac{1}{\gamma}\, \Phi_{lab}(E_\nu, \theta)\, dE_\nu\, \frac{d^2\Omega}{4\pi}\,, \qquad (3)$$

where $\gamma = 1/\sqrt{1 - \beta^2}$ is the time dilation factor and where E_ν and $\Omega \equiv (\theta, \varphi)$ now denote the energy and solid angle of the emitted (anti-)neutrino in the laboratory (lab) frame, θ being the angle of emission with respect to the beam axis. The boosted flux $\Phi_{lab}(E_\nu, \theta)$ is given by:

$$\Phi_{lab}(E_\nu, \theta) = \frac{\Phi_{cm}(E_\nu \gamma[1 - \beta \cos\theta])}{\gamma[1 - \beta \cos\theta]}\,. \qquad (4)$$

We consider a storage ring of total length L with a straight sections of length D. In the long-time, stationary regime, the mean number of ions in the storage ring is $\gamma\tau g$, where $\tau = t_{1/2}/\ln 2$ is the lifetime of the parent nuclei and g is the number of injected ions per unit time. The total number of neutrinos emitted per unit time from a portion $d\ell$ of the decay ring is

$$\frac{dN_\nu}{dt} = \gamma\tau\, g \times \frac{dW}{dt}\bigg|_{lab} \times \frac{d\ell}{L}\,. \qquad (5)$$

For simplicity, we consider a cylindrical detector of radius R and depth h, aligned with one the straight sections of the storage ring, and placed at a distance d from the latter. After integration over the useful decay path and over the volume of the detector, the total number of events per unit time is:

$$\frac{dN_{ev}}{dt} = g\tau nh \times \int_0^\infty dE_\nu\, \Phi_{tot}(E_\nu)\, \sigma(E_\nu)\,, \qquad (6)$$

where n is the number of target nuclei per unit volume, $\sigma(E_\nu)$ is the relevant neutrino-nucleus interaction cross-section, and where

$$\Phi_{tot}(E_\nu) = \int_0^D \frac{d\ell}{L} \int_0^h \frac{dz}{h} \int_0^{\bar\theta(\ell, z)} \frac{\sin\theta d\theta}{2}\, \Phi_{lab}(E_\nu, \theta)\,, \qquad (7)$$

with

$$\tan\bar\theta(\ell, z) = \frac{R}{d + \ell + z}\,. \qquad (8)$$

Large versus Small Ring configurations

The storage ring geometry is characterized by the length of the straight sections D and by its total length L. Below, we consider the cases of a small (SR) and a large (LR) ring configurations, characterized by (D_{SR}, L_{SR}) and (D_{LR}, L_{LR}) respectively. The results in both configurations can easily be related to one another by splitting the integral over the useful decay path $\int_0^{D_{LR}} \equiv \int_0^{D_{SR}} + \int_{D_{SR}}^{D_{LR}}$ in Eq. (7). Up to trivial $1/L$ factors, the LHS corresponds to the LR configuration and the first term on the RHS to the SR configuration. The remaining integral can be given a simple analytical estimate if one can neglect the angular dependence of the flux under the integral. This happens when the angle under which the detector is seen from the extremity of the SR decay path $\sim R/(d + D_{SR})$ is small compared to $1/\gamma$, i.e. to the typical opening angle of the boosted flux. In that case, we obtain, for the total flux (7):

$$\Phi_{tot}^{LR}(E_\nu) \simeq \frac{L_{SR}}{L_{LR}} \times \left\{ \Phi_{tot}^{SR}(E_\nu) + G\, \Phi_{lab}(E_\nu, \theta = 0) \right\}\,, \qquad (9)$$

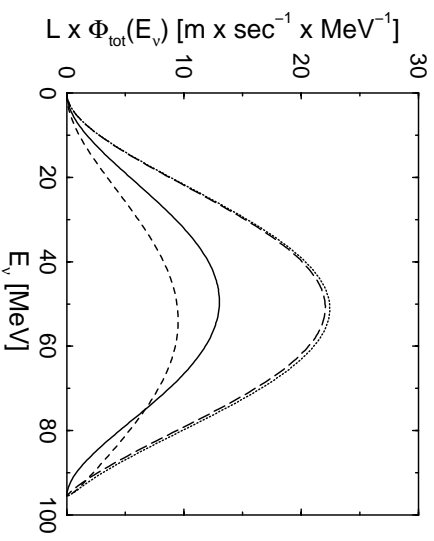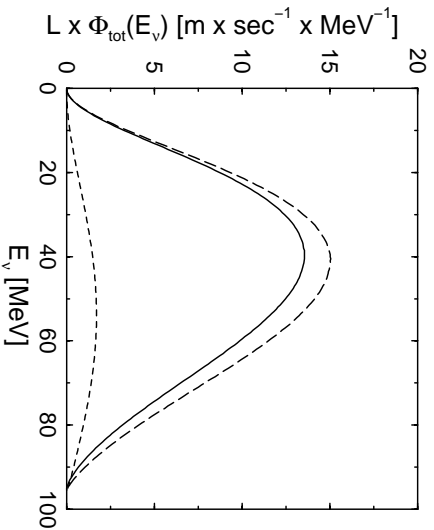L x Φ_tot(E_ν) [m x sec⁻¹ x MeV⁻¹]

E_ν [MeV]

FIG. 1: Neutrino fluxes scaled by the length of the storage ring $L \times \Phi_{tot}(E_\nu)$: The exact results obtained with Eqs.(7)-(8) with a small storage ring SR (solid lines) and a large storage ring LR (long-dashed lines) are shown. The left (right) figure shows the fluxes impinging on the small (large) detector (the sizes are given in Tables I and II). For the small detector (left), the LR result obtained with the analytical estimate (9) coincide with the exact result and is not represented here for clarity. For the large detector (right), it is also a very good approximation as shown by the dotted-line. The contribution $L \times G \times \Phi_{lab}(E_\nu, \theta = 0)$ is also presented (dashed lines). All fluxes are obtained with ^{18}Ne boosted at $\gamma = 14$.

where the geometrical factor G is given by:

$$G = \frac{R^2}{4 L_{SR}(d + D_{SR})}\left(1 - \frac{d + D_{SR}}{d + D_{LR}}\right).$$ (10)

The overall factor L_{SR}/L_{LR} in (9) simply accounts for the fact that the number of decaying ions per unit length is smaller in a larger storage ring, and the second term in brackets on the RHS represents the contribution from the longer useful straight section. Figure 1 shows a comparison between the exact flux obtained with Eqs.(7)-(8) in both the SR and the LR configurations, and the analytic estimate Eq. (9), for the two possible detector sizes considered in the following. We see that the analytical formula (9) works very well in the cases considered here. Besides, Figure 1 shows that the contribution from the longer decay path only brings a $\sim 10\%$ difference for the small detector and contributes a factor ~ 2 for the larger detector. This already shows that the main difference between the LR and SR fluxes comes from the geometrical factor $L_{SR}/L_{LR} \simeq 1/15$.

Using the approximate formula for the total fluxes, we obtain an approximate relation between the total number of events in the LR and SR configurations:

$$\frac{dN_{ev}}{dt}\Big|_{LR} \simeq \frac{L_{SR}}{L_{LR}} \times \left\{ \frac{dN_{ev}}{dt}\Big|_{SR} + \gamma^2(1+\beta)^2 F\, g\eta h \langle\sigma\rangle_\gamma \right\},$$ (11)

where we define the flux averaged cross section:

$$\langle\sigma\rangle_\gamma = \frac{\int_0^\infty dE_\nu\, \Phi_{cm}(E_\nu)\, \sigma(\gamma(1+\beta)E_\nu)}{\int_0^\infty dE_\nu\, \Phi_{cm}(E_\nu)}.$$ (12)

It is to be noted that, when the detector is placed close to the storage ring, as it is the case here, the total rate (6)

depends non-trivially on the geometry of the latter. For instance, as discussed above, we observe an approximate $1/L$ scaling at fixed D/L in the small detector case. This is in contrast with the case of a far detector considered so far, where the rate is simply proportional to the ratio D/L of the straight sections over the total length of the ring [33].

II. RESULTS

Here, we present charged-current neutrino interaction rates with various target nuclei as obtained from Eqs. (6)-(8) (Tables I and II). Four possible nuclei are taken as typical examples, namely deuteron, oxygen, iron and lead. The "small ring" we consider has 150 meter straight sections and 450 meter total length, while the "large ring" has 2.5 km straight sections and 7 km total length. The detectors are located at a distance 10 meters from the storage ring, to allow a maximum shielding of the induced background in the ring [29]. For the detector size we inspire ourselves on the kinds considered for the proposed ORLAND facility [18]. The transverse size is chosen so as to catch as much as possible of the boosted flux, which main contribution is concentrated in an opening angle $\sim 1/\gamma$. More precisely, we choose as typical dimensions (R-radius, h=depth): $R = 1.5$ m and $h = 4.5$ m. We also consider the case of a large (kiloton-type) water detector with $R = 4.5$ m and $h = 15$ m. Finally, we have to specify the number of parent ions g injected per unit time in the storage ring. According to the feasibility study [21], $2\times10^{13}\,^6$He/sec and $8\times10^{11}\,^{18}$Ne/sec could be produced with an ISOLDE technique, giving about $g_\nu = 10^{13}\,\bar{\nu}$/sec and $g_\nu = 5 \times 10^{11}\,\nu$/sec respectively [21]. An important

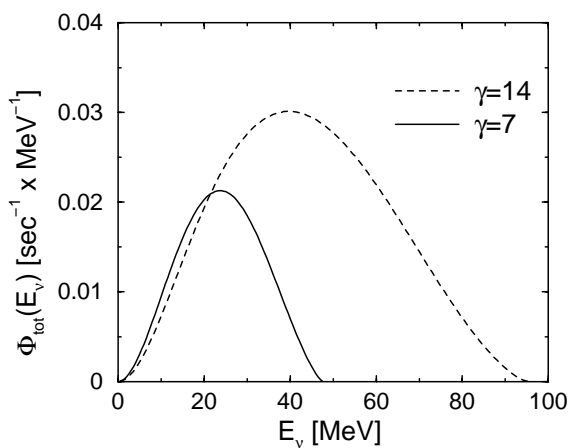L x Φ_tot(E_ν) [m x sec⁻¹ x MeV⁻¹]

E_ν [MeV]

FIG. 2: Neutrino fluxes $\Phi_{tot}(E_\nu)$ as a function of energy for ^{18}Ne nuclei boosted at $\gamma = 7$ and $\gamma = 14$. This corresponds to the small ring and small detector configuration.
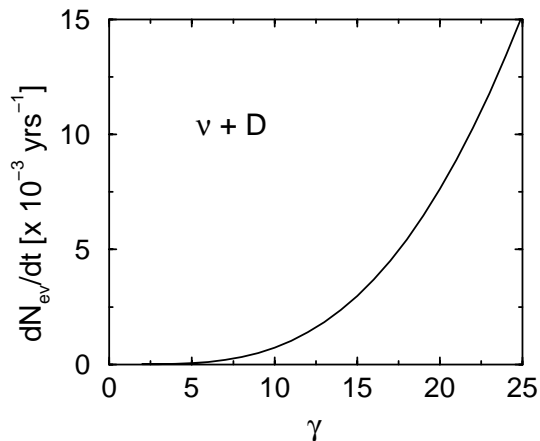

FIG. 3: The total rate for the reaction $\nu + D$ as a function of the boost factor γ. This corresponds to the small ring and small detector configuration.

feature of beta-beams is that the number and average energy of neutrinos entering the detector depend on the boost factor γ of the parent ion, which can be varied. We present results for two different values, namely $\gamma = 7$ (Table I) and $\gamma = 14$ (Table II). The corresponding neutrino fluxes are presented in Figure 2 and range up to about 50 and 100 MeV respectively. Note, in particular, that the $\gamma = 7$ spectrum covers the energy range of interest for supernova astrophysics.

Let us discuss the number of events shown in Tables I and II. The differences between the ν–induced versus $\bar{\nu}$–

induced reactions is a combined effect of the relative factor $g_\nu/g_{\bar{\nu}} = 1/20$ in the incoming fluxes and of the different interaction cross-sections: the ratio $\sigma(\nu + D)/\sigma(\bar{\nu} + D)$ is roughly 2 in the whole energy range considered here [9]; from [30], one can see that $\sigma(\nu + {}^{16}O)/\sigma(\bar{\nu} + {}^{16}O)$ is about 0.5 on average in the energy range relevant to the case $\gamma = 7$, namely 20 MeV $\lesssim E_\nu \lesssim$ 40 MeV, and about 1.5 on average in the range 40 MeV $\lesssim E_\nu \lesssim$ 80 MeV, relevant for the case $\gamma = 14$. The very low rates obtained for oxygen with $\gamma = 7$ despite the large detector size are due to the 15 MeV threshold in the interaction cross-section. Next, we observe that the suppression of the rates in the LR configuration as compared to the SR case for a given γ roughly corresponds to the geometrical factor L_{SR}/L_{LR}, as expected from the previous discussion. In fact, the difference between the LR and SR rates can be fully understood by means of the approximate relation Eq. (11). This formula can be used to rescale our results for other possible dimensions of the storage ring. To this aim, we give the relevant values of $\langle\sigma\rangle_\gamma$ in each case. When going from $\gamma = 7$ to $\gamma = 14$, the neutrino fluxes become more collimated and the typical energy of the neutrinos increases. This, together with the fact that the neutrino-nucleus interaction cross sections rapidly rise with the impinging neutrino energy, increases the number of events by more than an order of magnitude. Figure 3 illustrates the rapid rise of the total rates with increasing γ. Note that, in the present case, where the detector is relatively close to the storage ring, the total rates do not have a simple scaling with the detector size, due to the non-trivial angular dependence of the impinging neutrino flux.

To conclude, we see that, with the present set-up, the rates obtained at $\gamma = 7$ with a large storage ring are pretty low. This could, in principle, be improved by increasing the ions injection rate g in the storage ring. Therefore, it would be of interest to investigate whether higher injection rates could be obtained in future feasibility studies. As emphasized previously, the situation rapidly improves as γ is increased. Moreover, our results show that a small ring – with as long as possible straight sections – is the preferred configuration when working with a close detector. Our main result is that, with typical parameters available from existing studies [21], reasonable interaction rates can be achieved at a low-energy beta-beam facility. We think the present study is encouraging and we hope it will trigger further investigations, including, in particular, detailed simulations of the detectors.

[1] R. Davis, Phys. Rev. Lett. 12, 303 (1964).
[2] S.E. Woosley et al, Astrophys.J. 356, 272 (1990).
[3] A.B. Balantekin, Prog. Theor. Phys. Suppl. 146, 227 (2003).

Reaction	Ref.	Mass	$\langle\sigma\rangle_\gamma$	Small Ring	Large Ring
$\nu+$D	[9]	35	36.30	194	14
$\bar\nu+$D	[9]	35	23.16	2494	178
$\nu+^{16}$O	[30]	952	3.33	60	6
$\bar\nu+^{16}$O	[30]	952	5.04	2125	192
$\nu+^{56}$Fe	[31]	250	137.86	872	63
$\nu+^{208}$Pb	[32]	360	2931.24	7598	545

TABLE I: Number of events per year for $\gamma = 7$ in the small ($L_{SR} = 450$ m, $D_{SR} = 150$ m) and large ($L_{LR} = 7$ km, $D_{LR} = 2.5$ km) ring configurations. The detector is located at $d = 10$ m away from the ring and has dimensions $R = 1.5$ m and $h = 4.5$ m for the D (D$_2$O), ^{56}Fe and ^{208}Pb, and $R = 4.5$ m and $h = 15$ m for the case of ^{16}O (H$_2$O), where R is the radius and h is the depth of the detector. The corresponding masses are given in tons. We also give the flux averaged cross section $\langle\sigma\rangle_\gamma$ (see Eq. (12)) in units of 10^{-42} cm^2. The results in the large ring configuration can be precisely understood from those in the small ring configuration by means of the analytical estimate Eq. (11). The relevant cross-sections are taken from the indicated references. The results are obtained with 1 year = 3.2×10^7 s.

Reaction	Ref.	Mass	$\langle\sigma\rangle_\gamma$	Small Ring	Large Ring
$\nu+$D	[9]	35	184.47	2363	180
$\bar\nu+$D	[9]	35	96.03	25779	1956
$\nu+^{16}$O	[30]	952	174.28	6054	734
$\bar\nu+^{16}$O	[30]	952	102.00	82645	9453
$\nu+^{56}$Fe	[31]	250	1402.11	20768	1611
$\nu+^{208}$Pb	[32]	360	16310.16	103707	7922

TABLE II: Same as Table I for $\gamma = 14$.

[4] G.McLaughlin and G.M. Fuller, Astrophys. J. 455, 202 (1995).

[5] A. Heger et al, astro-ph/0307546.

[6] A.B. Balantekin and G.M. Fuller, J. Phys. G 29, 2513 (2003); astro-ph/0309519.

[7] Y.Z. Qian et al., Phys. Rev. C 55, 1532 (1997).

[8] I.N. Borzov and S. Goriely, Phys. Rev. C 62, 035501-1 (2000).

[9] K. Kubodera and S. Nozawa, Int. J. Mod. Phys. E 3, 101 (1994) and references therein.

[10] S. Ying, W. C. Haxton, and E. M. Henley, Phys. Rev. C 45, 1982 (1992); D.B. Kaplan, M.J. Savage, M.B. Wise, Phys. Lett. B 424, 390 (1998); M. Butler, J.-W.Chen, X. Kong, Phys. Rev. C 63, 035501 (2001), nucl-th/0008032; K. Kubodera, Nucl. Phys. Proc. Suppl. 100,30 (2001); M. Butler, J.-W. Chen, P. Vogel, Phys. Lett. B 549, 26 (2002), nucl-th/0206026; A.B. Balantekin and H. Yüksel, hep-ph/0307227.

[11] F. Osterfeld, Rev. Mod. Phys. 64, 491 (1992); and references therein.

[12] C. Volpe et al., Phys. Rev. C 62, 015501 (2000).

[13] R. Surman and J. Engel, Phys. Rev. C 58, 2526 (1998).

[14] E. Kolbe et al., Phys. Rev. C 52, 3437 (1995); N. Auerbach, N. Van Giai and O.K. Vorov, Phys. Rev. C 56, R2368 (1997); S.K. Singh, N.C. Mukhopadyhay and E. Oset, Phys. Rev. C 57, 2687 (1998); S.L. Mintz and M. Pourkaviani, Nucl. Phys. A 594, 346 (1995); E. Kolbe, K. Langanke and P. Vogel, Nucl. Phys. A 613, 382 (1997);

A.C. Hayes and I.S. Towner, Phys. Rev. C 61, 044603 (2000); C. Volpe et al., Phys. Rev. C 62, 015501 (2000); N. Auerbach and B.A. Brown, Phys. Rev. C 65, 024322 (2002); N. Jachowicz et al., Phys. Rev. C 65, 025501 (2002).

[15] S.E. Willis et al., Phys. Rev. Lett. D 4, 522 (1980).

[16] C.Athanassopoulos and the LSND collaboration, Phys. Rev. C 56, 2806 (1997); M.Albert et al., Phys. Rev. C 51, R1065 (1995); C.Athanassopoulos and the LSND collaboration, Phys. Rev. C 55,2078 (1997); D.A.Krauker et al., Phys. Rev. C 45, 2450 (1992); R.C.Allen et al., Phys. Rev. Lett. 64, 1871 (1990); B.E.Bodmann and the KARMEN collaboration, Phys. Lett. B332, 251 (1994); J.Kleinfeller et al., in Neutrino 96, eds. K.Enquist, H.Huitu and J.Maalampi (World Scientific Singapore, 1997).

[17] E. Kolbe, K. Langanke and G. Martinez-Pinedo, Phys. Rev. C 60, 052801 (1999).

[18] F.T. Avignone et al., Phys. Atom. Nucl.63, 1007 (2000); see http://www.phy.ornl.gov/orland/.

[19] See http://www.pas.rochester.edu/ ksmcf/minerva/.

[20] P. Zucchelli, Phys. Lett. B 532, 166 (2002).

[21] B. Autin et al., J. Phys. G 29, 1785 (2003); physics/0306106. See also http://beta-beam.web.cern.ch/beta-beam/.

[22] C.K. Jung, Proceedings of the "Next generation Nucleon Decay and Neutrino Detector (NNN99) Workshop", September 23-25, 1999, Stony Brook, New York;

hep-ex/0005046.

[23] M. Mezzetto, J. Phys. G **29**, 1771 (2003); hep-ex/0302007.

[24] J. Burguet-Castell *et al.*, IFIC/03-55; hep-ph/0312068.

[25] C. Volpe, to be published in J. Phys. G; hep-ph/0303222.

[26] G.C. McLaughlin and C. Volpe, to be published in Physics Letters B; hep-ph/0312156.

[27] See http://www.gsi.de/.

[28] K.S. Krane, *"Introductory Nuclear Physics"*, Ed. John Wiley and Sons (1998).

[29] M. Magistris and M. Silari, CERN-TIS-2003-017-TN.

[30] E. Kolbe, K. Langanke, P. Vogel, Phys. Rev. D **66**, 013007 (2002); W.C. Haxton, Phys. Rev. D **36**, 2283 (1987).

[31] E. Kolbe and K. Langanke, Phys. Rev. C **63**, 025802 (2001).

[32] J. Engel, G.C. McLaughlin, C. Volpe, Phys. Rev. D **67**, 013005 (2003).

[33] For a distant detector $(d \gg L, D, h)$, one has simply: $\Phi_{tot}(E\nu) \simeq \Phi_{lab}(E_\nu, \theta = 0) \frac{D}{L} \frac{S}{4\pi d^2}$, where $S = \pi R^2$ is the transverse area of the detector. Similarly, one obtains, for the rate: $\frac{dN_{e\nu}}{dt} \simeq g \frac{D}{L} \frac{N_{target}}{4\pi d^2} \gamma^2 (1 + \beta)^2 \langle \sigma \rangle_\gamma$, where $N_{target} = n\pi R^2 h$ is the total number of target nuclei.